Chaos and strange attractors in coupled oscillators with energy-preserving nonlinearity

2008 J. Phys. A: Math. Theor. 41 255101

(http://iopscience.iop.org/1751-8121/41/25/255101)

IOP PUBLISHING JOURNAL OF PHYSICS A: MATHEMATICAL AND THEORETICAL

J. Phys. A: Math. Theor. **41** (2008) 255101 (17pp) doi:10.1088/1751-8113/41/25/255101

Chaos and strange attractors in coupled oscillators with energy-preserving nonlinearity

F Adi-Kusumo[1], J M Tuwankotta and W Setya-Budhi

Analysis and Geometry Group, Faculty of Mathematics and Natural Sciences, Bandung Institute of Technology, Jl. Ganesa no. 10 Bandung, Indonesia

E-mail: fajar_ak@math.itb.ac.id, theo@math.itb.ac.id and wono@math.itb.ac.id

Received 17 December 2007, in final form 5 April 2008
Published 22 May 2008
Online at stacks.iop.org/JPhysA/41/255101

Abstract

We present an analysis for a particular singularly perturbed conservative system. This system comes from the normal form of two coupled oscillator systems with widely-separated frequencies and energy-preserving nonlinearity. The analysis is done in this paper for a degenerate case of such a system, while the generic one has been treated in the literature. To understand the relation with the strong resonance case, we have computed the normal form of the 2:1 resonance, and found that the latter is contained in our system. We present a theorem that gives the existence of a nontrivial equilibrium for a general singularly perturbed conservative system. We detect that the nontrivial equilibrium undergoes two Hopf bifurcations. Furthermore, the periodic solutions created through these Hopf bifurcations undergo a sequence of period doubling bifurcations. This leads to the presence of chaotic dynamics through Shil'nikov bifurcation of a homoclinic orbit. Also, we measure the size of the chaotic attractor which is created in our system.

PACS numbers: 02.60.Lj, 05.45.−a, 02.30.Oz
Mathematics Subject Classification: 34C15, 37D45, 37G05, 37G15

1. Introduction

It is well known that resonances are responsible for the nontrivial dynamics in a system of two coupled oscillators (see [1, 9, 16, 19, 20]). One of those dynamics is the energy transfer between oscillators. In strong resonance cases (such as 2 : 1 resonance), this happens more dramatically in comparison with the higher order ones. See, for example, in [6, 19] for strong resonances; for higher order resonances, see [9, 16, 17, 20].

[1] Permanent address: Jurusan Matematika, FMIPA, Universitas Gadjah Mada, Sekip Utara Yogyakarta 55281, Indonesia.

Starting from the year 1990, people are looking at an extreme type of higher order resonance (think of $1 : \varepsilon$ resonance, where $\varepsilon \ll 1$). See, for example, in [2, 3, 12–15, 22–24]. One of conclusions from those studies that this type of resonance, which is also called a widely separated frequency case, the dynamics of the system is rather different from an ordinary higher order resonance.

Our study in this paper is motivated by the results in [23, 24]. In those papers, a system of coupled oscillators with widely separated frequencies is studied. Apart from having the assumption on the frequencies, the author there also assumes that the nonlinearity of the system preserves energy which is represented by the distance to the origin. Under these two assumptions, the system produces interesting dynamics.

In application, the system in [23, 24] is a generalization of a mathematical model in atmospheric research which is called ULFV (ultra-low frequency variability) model. The model represents a long-time behavior of the interaction patterns in atmosphere. The normal form in [23, 24] can be seen as a singularly perturbed conservative system. This is due to the assumption on the nonlinearity being energy preserving. As a consequence, the dynamics is decomposed into two time scales, namely slow–fast dynamics.

One of the interesting dynamics that occur is the existence of a sequence of period-doubling bifurcations. The bifurcations usually lead chaotic dynamics of a system, but in [23] it does not seem to be the case. Another interesting dynamics is the so-called Neimark–Sacker bifurcation which produces torus solutions. The break-up of this torus solution usually implies interesting (most of the time chaotic) dynamics, see [24].

The study in [23, 24] is concentrated on the generic cases (namely all of the parameters in the system admit general values). In this paper we will deal with one of the degeneracies that arise in the system. This degeneracy can be induced by the presence of a particular discrete symmetry which is also abundant in nature. Preliminary results in this case, which are for the energy-preserving system have been shown in [23]. One of the complications that arise immediately in the degenerate case is that we will have to deal with a slow manifold which is entirely not normally hyperbolic.

Another motivation for studying this degenerate system is the following. The system contains the normal form for a totally different resonance, i.e. the 2:1 resonance . The latter is the strongest resonance in a system of two coupled oscillators. Even in the Hamiltonian case, this resonance produces a large energy exchange between the oscillators. At the end, it leads to irregular and chaotic behaviors of the system. This result is a confirmation of the previous results of the widely-separated frequency case, see [2, 3, 12–15].

1.1. Summary of the result

Our system and the normal form in [23, 24] are examples of the *singularly perturbed conservative system*. Thus, our dynamical system is conservative when the perturbation parameter is set to zero. The conserved quantity in our system takes the form of an invariant sphere in $\mathbb{R}^3$. The perturbed flow creates the dynamics transversal to these spheres.

It is evident that our system admits two equilibria, i.e. the trivial and the nontrivial ones. The stability analysis for the trivial equilibrium can be deduced from linear analysis. The nontrivial one however is more cumbersome to use linear analysis. We have applied the asymptotic method to deduce that stability of the nontrivial equilibrium. This nontrivial equilibrium undergoes Hopf bifurcation. Furthermore, the periodic solution created by this Hopf bifurcation undergoes a sequence of periodic doubling bifurcations. Moreover, a homoclinic orbit is created and it fits Shil'nikov condition for chaos.

The analysis of the fully perturbed system which is mentioned above, is done using the numerical continuation toolbox MATCONT, see [5]. The existence of the nontrivial equilibrium then becomes crucial. Although in our system it is evident that such an equilibrium exists, in this paper we provide a theorem that gives the existence for such an equilibrium for a more general setting (see theorem 3.1). The proof is based on the implicit function theorem and the Taylor formula without the remainder.

It is interesting to note that the system which is analyzed here also contains the normal form of the system in [23, 24] at 2:1 resonance. This is a completely different resonance—namely one of the strong resonances (see appendix B). This suggests that an extreme type of higher order resonances should be seen as first-order resonances.

We have found difficulty in providing a complete numerical bifurcation analysis for the case $\delta < 0$. The 2:1 resonance case explained in appendix B is in this region. In our system, a complete analysis can be done only in the parameter regions in $\delta > 0$. Some preliminary results for the case $\delta < 0$ are presented in the last section, but further study is necessary for this case.

2. Formulation of the system

Let us now consider a system of ordinary differential equations in $\mathbb{R}^3$:

$$\begin{aligned} \dot{r} &= \delta x r + \varepsilon \kappa_1 r \\ \dot{x} &= \Omega y - \delta r^2 - \varepsilon \kappa_2 x \\ \dot{y} &= -\Omega x - \varepsilon \kappa_2 y \end{aligned} \tag{2.1}$$

with $\Omega = \alpha x + \beta y + \omega$. Following [23, 24], we assume $\kappa_1, \kappa_2 > 0, \omega > 0, \beta < 0$ while $\delta \neq 0$. This is not too much of a restriction to the system since using the symmetries in the system we can reconstruct the dynamics for the other part of the parameter space (see [23, 24] for details). In contrast to [23, 24], in this paper we choose $\alpha = 0$.

Note that the system (2.1) is a normal form of a system of coupled oscillators: $\dot{\boldsymbol{\xi}} = A\boldsymbol{\xi} + \boldsymbol{F}(\boldsymbol{\xi})$ where $\boldsymbol{F}$ is a homogeneous quadratic polynomial. The linear part of this system consists of oscillations with frequencies having the ratio of $1 : \varepsilon$. In appendix B we show that the normal of the system in the 2:1 resonance case is contained in system (2.1).

2.1. Notes for the energy-preserving part of system (2.1)

For $\varepsilon = 0$ the system (2.1) is called the energy-preserving system. All solutions of the system except for the trivial equilibrium lie on an invariant sphere. Dynamics of the system on the projecting plane of the sphere has been shown in [23]. In that paper, the author shows the change of the dynamics when the radius of the sphere is changed.

We will give some notes about the dynamics of the unperturbed system related to the results in [23]. The notes are not stated explicitly in [23] but they are necessary for understanding the connection between the dynamics of the unperturbed system which preserves the energy and the dynamics of the perturbed system which will be done in this paper.

For $\varepsilon = 0$ the system (2.1) has two manifolds of equilibria: one lies in the plane $r = 0$ and the other in the plane $x = 0$. In the plane $r = 0$, the parametrization of the manifold is

$$(r, x, y) = \left(0, x_o, -\frac{\omega}{\beta}\right), \qquad x_o \in \mathbb{R}. \tag{2.2}$$

The other manifold of equilibria is

$$(r, x, y) = \left(\sqrt{\frac{(\beta y_o + \omega) y_o}{\delta}}, 0, y_o \right). \tag{2.3}$$

We refer to [23] or [24] for the stability analysis of those equilibria. Solutions of the system in this case lie on an invariant sphere, so we can reduce the dimension of the system by projecting the upper half-sphere into the horizontal plane. By varying the radius of the sphere R, there are three bifurcation points, $R_1 = -\omega/\beta$ and

$$R_2 = -\frac{\omega}{2(\beta + \delta)} \sqrt{-\frac{\beta + \delta}{\delta}}.$$

All possible topologically different phase portraits of the reduced system (2.1) can be seen in [23].

From figure 4 in [23], the author found a simultaneous saddle-node and homoclinic bifurcations. They occur at the bifurcation point R_1 for $\delta > -\beta/2$. The other homoclinic bifurcations at R_1 also occur for $0 < \delta < -\beta/2$ and $\delta < 0$. At the bifurcation point R_2, a saddle node bifurcation occurs in the system.

3. On singularly perturbed conservative systems

3.1. Some notations

In the following section we will show the existence of the equilibrium of the singularly perturbed conservative system in a more general setting. Let us introduce some notations to facilitate our analysis. For a vector-valued function $\boldsymbol{F}$, F_k represents the kth component of $\boldsymbol{F}$, while $\boldsymbol{F}_k$ represents the vector-valued functions consisting of the first k components of $\boldsymbol{F}$. By $D_{\xi}\boldsymbol{F}$ we mean differentiation with respect to the spatial coordinate $\boldsymbol{\xi}$. The ∇H is the gradient vector of the real-valued function H. We will also use a notation for partial differentiation with respect to ε, which is $\frac{\partial}{\partial \varepsilon}$.

Let us now consider a slightly more general situation. Consider $\mathbb{R}^n$ with coordinate $\boldsymbol{\xi} = (\xi_1, \ldots, \xi_n)$. Consider a one-parameter family of C^k-vector fields $\boldsymbol{F} : \mathbb{R}^n \times (-\varepsilon_\circ, \varepsilon_\circ) \to \mathbb{R}^n$, for some real numbers $0 < \varepsilon_\circ \ll 1$ and $k \in \mathbb{N}$. Using $t \in \mathbb{R}$ as the time variable, the corresponding system of ordinary differential equations is

$$\dot{\boldsymbol{\xi}} = \boldsymbol{F}(\boldsymbol{\xi}, \varepsilon), \tag{3.1}$$

where the dot denotes the derivation with respect to t.

Furthermore, we assume:

(i) there exists a C^k-function $H : \mathbb{R}^n \to \mathbb{R}$ such that $(\nabla H(\boldsymbol{\xi}))^T \cdot \boldsymbol{F}(\boldsymbol{\xi}, 0) = 0$ for all $\boldsymbol{\xi} \in \mathbb{R}^n$, and
(ii) if $\varepsilon \neq 0$, $(\nabla H(\boldsymbol{\xi}))^T \cdot \boldsymbol{F}(\boldsymbol{\xi}, 0) \neq 0$ for some $\boldsymbol{\xi} \in \mathbb{R}^n$.

If $(\nabla H(\boldsymbol{\xi}))^T \cdot \boldsymbol{F}(\boldsymbol{\xi}, \varepsilon)$ is sign-definite, then the invariant sets of the system can be characterized by looking at the critical sets of the function H. A more exciting situation is if $(\nabla H(\boldsymbol{\xi}))^T \cdot \boldsymbol{F}(\boldsymbol{\xi}, \varepsilon)$ is not sign-definite. Then there exists $\boldsymbol{\xi}$ such that $(\nabla H(\boldsymbol{\xi}))^T \cdot \boldsymbol{F}(\boldsymbol{\xi}, \varepsilon) = 0$. Let us define

$$\mathcal{C} = \{\boldsymbol{\xi} \in \mathbb{R}^n \,|\, (\nabla H(\boldsymbol{\xi}))^T \cdot \boldsymbol{F}(\boldsymbol{\xi}, \varepsilon) = 0\}, \tag{3.2}$$

and we assume that, for all $\boldsymbol{\xi}$ in $\mathcal{C}$

$$D_{\xi}\left(\nabla H(\boldsymbol{\xi})\right) \cdot \boldsymbol{F}(\boldsymbol{\xi}, \varepsilon) + D_{\xi}\boldsymbol{F}(\boldsymbol{\xi}, \varepsilon) \cdot \nabla H(\boldsymbol{\xi}) \neq 0. \tag{3.3}$$

By this we have that $\mathcal{C}$ is an $(n-1)$-dimensional (or a codimension-one) manifold in $\mathbb{R}^n$. This implies that $\mathcal{C}$ separates $\mathbb{R}^n$ into the expanding part where $(\nabla H(\boldsymbol{\xi}))^T \cdot \boldsymbol{F}(\boldsymbol{\xi}, \varepsilon) > 0$ and the contracting part where $(\nabla H(\boldsymbol{\xi}))^T \cdot \boldsymbol{F}(\boldsymbol{\xi}, \varepsilon) < 0$. If an equilibrium exists, it should lie on $\mathcal{C}$.

Let us now look for the conditions for the existence of an equilibrium for the system (3.1). Let us denote by $\boldsymbol{F}^\circ(\boldsymbol{\xi})$ the vector field $\boldsymbol{F}(\boldsymbol{\xi}, 0)$ and by $\boldsymbol{F}^1(\boldsymbol{\xi})$ the vector field $\frac{\partial \boldsymbol{F}}{\partial \varepsilon}(\boldsymbol{\xi}, \varepsilon)$ evaluated at $\varepsilon = 0$. Recall that there exists a real-valued function H defined in an open neighborhood of $\boldsymbol{\xi}_\circ$, such that $(\nabla H(\boldsymbol{\xi}))^T \boldsymbol{F}^\circ(\boldsymbol{\xi}) = 0$. Furthermore, we write $G(\boldsymbol{\xi}) = (\nabla H(\boldsymbol{\xi}))^T \boldsymbol{F}^1(\boldsymbol{\xi})$, $K = \ker(D_{\boldsymbol{\xi}} \boldsymbol{F}^\circ(\boldsymbol{\xi}_\circ))$ and $L = \ker(D_{\boldsymbol{\xi}} G(\boldsymbol{\xi}_\circ))$.

Theorem 3.1. *We assume that there exists $\boldsymbol{\xi}_\circ \in \mathbb{R}^n$ such that the following conditions hold:*

(A_1) $\boldsymbol{F}^\circ(\boldsymbol{\xi}_\circ) = 0$.
(A_2) $G(\boldsymbol{\xi}_\circ) = 0$.
(A_3) $K \cap L = \{\mathbf{0}\}$.

Then we have the following conclusions.

(i) There is a C^k-curve in a neighborhood $V_{\boldsymbol{\xi}_\circ}$ of $\boldsymbol{\xi}_\circ$, i.e. $h \in \mathbb{R}, h \mapsto \boldsymbol{\xi}(h)$, such that $\boldsymbol{F}^\circ(\boldsymbol{\xi}(h)) = 0$, $H(\boldsymbol{\xi}(h)) = h$, and the tangent space $T_{\boldsymbol{\xi}_\circ}\mathcal{E}$ is equal to K, where $\mathcal{E} = \{\boldsymbol{\xi}(h) \mid \boldsymbol{F}^\circ(\boldsymbol{\xi}(h)) = 0, h \in J \subset \mathbb{R}\}$.
(ii) There is a C^{k-1}-curve (parametrized by ε) $\gamma : I \to \mathbb{R}^n$, where I is an open interval around 0, and there exists an open neighborhood V of $\boldsymbol{\xi}_\circ \in \mathbb{R}^n$, such that $\gamma(0) = \boldsymbol{\xi}_\circ$ and, for every nonzero $\varepsilon \in I$, $\boldsymbol{F}(\gamma(\varepsilon), \varepsilon) = 0$.

Remark 3.2. The proof for theorem 3.1 (which is presented in the appendix of this paper) was suggested by Professor J J Duistermaat from Universiteit Utrecht. The original version of theorem 3.1 (see [21]) assumes a stronger condition on the critical point $\boldsymbol{\xi}_\circ$ which is the following. Suppose we restrict the flow on a level set of H containing $\boldsymbol{\xi}_\circ$. Then as a critical point of the restricted vector field, $\boldsymbol{\xi}_\circ$ is assumed to be hyperbolic. The current version of theorem 3.1 does not exclude the possibility that $\boldsymbol{\xi}_\circ$ is a nonhyperbolic point (for example, a center point). However, by assuming hyperbolicity, we can also derive the stability of the equilibrium by using the center manifold theorem. The first conclusion in theorem 3.1 is a refinement of the discussion in [21]. There we use the topological argument to conclude the existence of the parametrized family of critical points of the conservative system, following [8, 10]. However, the topological argument applies only in the case the dimension n is an odd number.

Remark 3.3. In the case where $\boldsymbol{\xi}_\circ$ is a more degenerate critical point, one needs to be a bit careful with the conclusion. For instance in the case where $K \cap L \neq \{0\}$, one needs to apply some blow-up transformation there to see the complete picture of the dynamics. See for instance [18].

4. The analysis for the perturbed system

Let us now consider equation (2.1) for $\varepsilon \neq 0$. Recall that we have assumed $\kappa_1 > 0, \kappa_2 > 0$, $\omega > 0$, while $\beta < 0$. The system (2.1) can be written as $\dot{\boldsymbol{\xi}} = \boldsymbol{F}^\circ(\boldsymbol{\xi}) + \varepsilon \boldsymbol{F}^1(\boldsymbol{\xi})$ where $\boldsymbol{\xi} = (r, x, y)^T$, $\boldsymbol{F}^\circ(\boldsymbol{\xi}) = (\delta x r, \Omega(y)y - \delta r^2, -\Omega(y)x)^T$ and $\boldsymbol{F}^1(\boldsymbol{\xi}) = (\kappa_1 r, -\kappa_2 x, -\kappa_2 y)^T$. For the manifold $\mathcal{C}$ we have the cone $\mathcal{C} = \{(r, x, y) | \kappa_1 r^2 - \kappa_2(x^2 + y^2) = 0\}$.

In order to apply theorem 3.1 we need to find a point $\boldsymbol{\xi}_\circ \in \mathbb{R}^n$ which satisfies the three conditions. Geometrically, condition (A_1) means that $\boldsymbol{\xi}_\circ$ is an equilibrium of the unperturbed system of (2.1). Condition (A_2) means that $\boldsymbol{\xi}_\circ$ must lie on $\mathcal{C}$. Thus we need to look for the intersection point between $\mathcal{C}$ and the manifolds of equilibria in (2.2), or between $\mathcal{C}$ and the

manifolds of equilibria in (2.3). Condition (A_3) gives us the transversality condition of the intersection.

In our case, we conclude that if the intersection point exists, then the intersection is always transversal. The intersection point does not exist in two cases: if $\delta = 0$ or if $\kappa_1\beta - \kappa_2\delta = 0$. The location of the nontrivial equilibrium is

$$r_o = \sqrt{\frac{\kappa_1\kappa_2(\omega^2\delta^2 + \varepsilon^2(\kappa_1\beta - \kappa_2\delta)^2)}{\delta^2(\kappa_1\beta - \kappa_2\delta)^2}}, \qquad x_o = -\frac{\varepsilon\kappa_1}{\delta}, \qquad y_o = -\frac{\kappa_1\omega}{\kappa_1\beta - \kappa_2\delta}. \tag{4.1}$$

4.1. Stability analysis for the nontrivial equilibrium

To analyze the stability of the nontrivial equilibrium, we assume that δ is a nonzero parameter and $\beta\kappa_1 - \delta\kappa_2$ is nonzero. Note that the nontrivial equilibrium depends continuously on ε. Thus, the matrix of the linearized vector field of (2.1) around the equilibrium also depends continuously on ε. As a consequence, the eigenvalues of the matrix also depend continuously on ε. Let us write the formal expansion for the eigenvalue:

$$\lambda = \tilde{\lambda}_0 + \varepsilon\tilde{\lambda}_1 + \varepsilon^2\tilde{\lambda}_2 + \cdots. \tag{4.2}$$

Substituting (4.2) into the characteristic equation, we compute $\tilde{\lambda}_k, k = 0, 1, 2, \ldots,$ subsequently and then we have three eigenvalues, $\lambda = \lambda_1, \lambda = \lambda_2$ and $\lambda = \lambda_3$. The eigenvalues are, up to $\mathcal{O}(\varepsilon^2)$:

$$\begin{aligned} \lambda_1 &= \varepsilon\frac{2\kappa_1(\beta\kappa_1 - \delta\kappa_2)}{\beta\kappa_1 + (2\kappa_1 + \kappa_2)\delta} \\ \lambda_{2,3} &= \pm\frac{\omega\sqrt{-\kappa_2\delta(\beta\kappa_1 + (2\kappa_1 + \kappa_2)\delta)}}{\beta\kappa_1 - \delta\kappa_2} + \frac{1}{2}\varepsilon\left(\frac{(\beta\kappa_1 - \delta\kappa_2)\beta\kappa_1 - 2\kappa_2\delta^2(\kappa_1 + \kappa_2)}{\delta(\beta\kappa_1 + (2\kappa_1 + \kappa_2)\delta)}\right). \end{aligned} \tag{4.3}$$

4.1.1. Hopf bifurcation of the equilibrium. Recall that we have assumed $\beta < 0$ (following [23, 24]). Let us now consider the domain on the (δ, β) plane, which is on the right of the line l, i.e. where $\beta\kappa_1 + (2\kappa_1 + \kappa_2)\delta > 0$. If $\delta > 0$ then the eigenvalues $\lambda_{2,3}$ in (4.3) are complex.

Let us now look at the $\mathcal{O}(\varepsilon)$ term of $\lambda_{2,3}$. These terms are zero if

$$\beta = \frac{\kappa_2 + \sqrt{9\kappa_2^2 + 8\kappa_1\kappa_2}}{2\kappa_1}\delta \qquad \text{or} \qquad \beta = \frac{\kappa_2 - \sqrt{9\kappa_2^2 + 8\kappa_1\kappa_2}}{2\kappa_1}\delta. \tag{4.4}$$

Lemma 4.1. *In the neighborhood of (4.4), the nontrivial equilibrium undergoes Hopf bifurcation.*

Proof. Consider $\delta > 0$. It remains to show that (4.4) occurs in the domain where $\beta\kappa_1 + (2\kappa_1 + \kappa_2)\delta > 0$. Note that

$$\sqrt{9\kappa_2{}^2 + 8\kappa_1\kappa_2} = \sqrt{(3\kappa_2 + 4\kappa_1)^2 - 16\kappa_1\kappa_2 - 16\kappa_1{}^2}.$$

Thus

$$\frac{\sqrt{9\kappa_2{}^2 + 8\kappa_1\kappa_2} - \kappa_2}{2\kappa_1} < \frac{4\kappa_1 + 2\kappa_2}{2\kappa_1},$$

which completes the proof. The proof for $\delta < 0$ can be done similarly. □

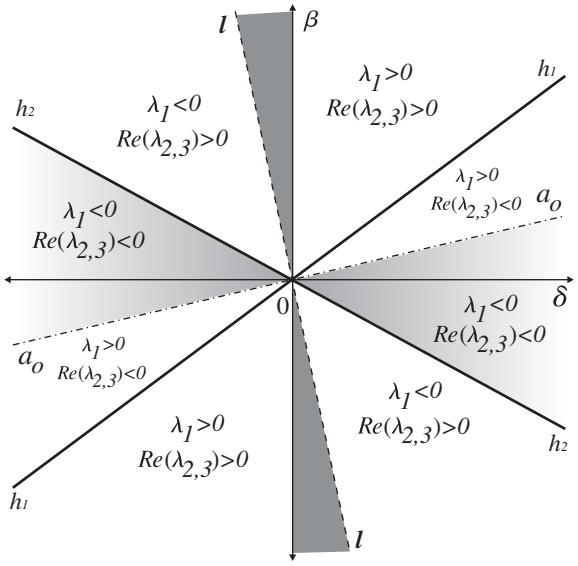

Figure 1. In this figure we have plotted the bifurcation sets for the nontrivial equilibrium. The line represented by $a_\circ$ is the line $\beta\kappa_1 - \delta\kappa_2 = 0$. On this line the nontrivial equilibrium goes to infinity. The lines h_1 and h_2 are the Hopf lines where the nontrivial equilibrium undergoes the Hopf bifurcation. The expressions for these Hopf lines are derived by analyzing (4.3). In the neighborhood of the line l: $\beta\kappa_1 + (2\kappa_1 + \kappa_2)\,\delta = 0$, the asymptotic in (4.3) is no longer valid.

Let us denote the line

$$\beta = \frac{\kappa_2 + \sqrt{9\kappa_2^2 + 8\kappa_1\kappa_2}}{2\kappa_1}\delta$$

by h_1, and

$$\beta = \frac{\kappa_2 - \sqrt{9\kappa_2^2 + 8\kappa_1\kappa_2}}{2\kappa_1}\delta$$

by h_2. These two lines, i.e. h_1 and h_2, are plotted in figure 1. From lemma 4.1 we know that on these lines, the nontrivial equilibrium undergoes Hopf bifurcations. The stability result for the nontrivial equilibrium is presented in figure 1.

4.1.2. The complement of the domain of validity for the asymptotic. There are two domains where the asymptotic for the eigenvalues (4.3) fails, i.e. the neighborhood of $\beta\kappa_1 + (2\kappa_1 + \kappa_2)\delta = 0$ (in figure 1, this is denoted by the line l) and the neighborhood of $\delta = 0$. Let us now define a new parameter

$$\nu\varepsilon^q = \beta\kappa_1 + (2\kappa_1 + \kappa_2)\delta \tag{4.5}$$

where q is a rational number to be determined. Substituting (4.5) into (4.3) and using the so-called *significant degeneracy* which is well known in singular perturbations, we derive that a suitable value for q is $\frac{2}{3}$. The same technique can be applied to the neighborhood of $\delta = 0$. We conclude with the following lemma.

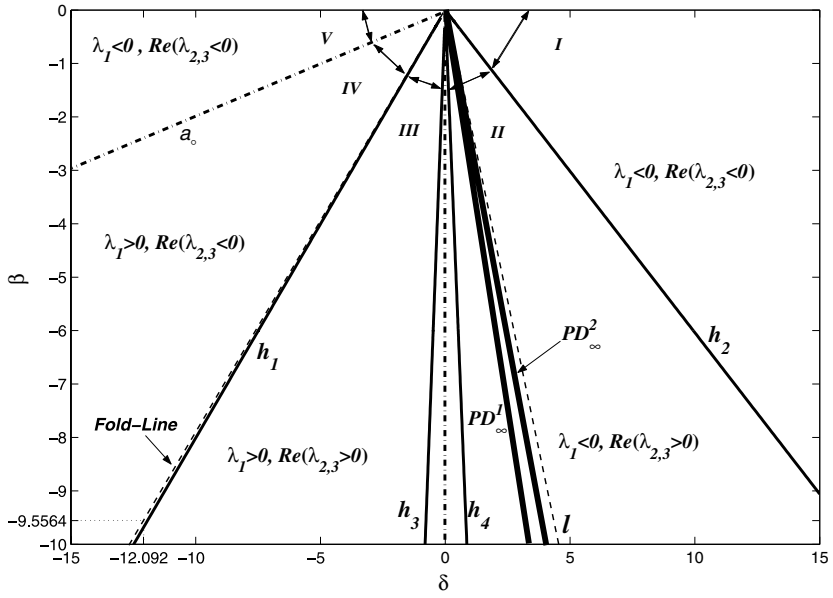

Figure 2. In this figure we have plotted the bifurcation sets which correspond to the nontrivial equilibrium of (4.1). These sets are obtained numerically. There are five special lines in the diagram that have been added. The line $a_\circ$ corresponds to the situation where the equilibrium goes to infinity. The line l corresponds to the neighborhood where the asymptotic for the eigenvalues (4.3) is not valid. The line PD^1_∞ and the line PD^2_∞ indicate the locations of the neighborhood where we expect to find homoclinic solutions. The last special line is the fold line at $\delta < 0$.

Lemma 4.2. *The asymptotic (4.3) is not valid on an* $\mathcal{O}(\varepsilon^{\frac{2}{3}})$ *neighborhood of the line* l *and an* $\mathcal{O}(\varepsilon^{\frac{2}{3}})$ *neighborhood of the* β*-axis.*

Remark 4.3. The situation in the neighborhood of the line l is rather interesting since this corresponds to the situation where $\boldsymbol{\xi}_\circ$ has three zero eigenvalues. This is a highly degenerate situation and further study is necessary to describe *the complete unfoldings* of the point. This is a topic of our future research. Note that in this paper, as $\varepsilon \neq 0$ all the degeneracies are removed, thus all the eigenvalues of the nontrivial equilibrium have nonzero real parts. Some preliminary result which is found numerically is presented in the following section.

5. Bifurcation analysis for the perturbed system

In this section, we present the bifurcations analysis for our system. We have used the Matlab continuation toolbox MATCONT (see [5]). For the numerical data we have used $\omega = 3, \kappa_1 = 5, \kappa_2 = 1, \varepsilon = 0.05$ and $\beta = -6$. We start with $\delta = 12$. By decreasing δ, we perform a one-parameter continuation of the nontrivial equilibrium. As predicted in the preceding section, we found a Hopf bifurcation at $\delta = 9.936\,110\ldots$, at which a stable periodic solution is created afterward.

Furthermore, we found a second Hopf bifurcation at $\delta = 0.519\,028\ldots$. This Hopf bifurcation produces an unstable periodic solution as we increase δ through the bifurcation point. Then we perform a two-parameter continuation (using δ and β) of these Hopf points. The results are plotted in figure 2. The two lines which are named h_2 and h_4, are the lines

Table 1. In this table we have listed the first five values of δ where the period-doubling occurs, when the period of the periodic solution is larger than 45, for various β.

$\beta =$	-3	-4	-5	-6	-9
δ	1.025532	1.371639	1.709219	2.057458	3.086188
	1.025788	1.366050	1.709640	2.049076	3.073640
	1.025730	1.368218	1.709459	2.052326	3.078495
	1.025729	1.367376	1.709550	2.051063	3.076595
	1.025732	1.367568	1.709547	2.051570	3.077030

where the first and the second Hopf bifurcations occur, respectively. Similarly for $\delta < 0$, we produce the two Hopf lines, i.e. h_1 and h_3.

To understand the dynamics of system (2.1), we consider five regions in figure 2:

- Region I: between the line h_2 and the δ-axis;
- Region II: between the line h_2 and the line h_4;
- Region III: between the line h_1 and the line h_3;
- Region IV: between the line $a_\circ$ and the line h_1;
- Region V: between the line $a_\circ$ and the δ-axis.

We remark that the region between h_3 and h_4 is excluded from our analysis due to the failure of the asymptotic (see also lemma (4.2)).

Dynamics in regions I and V are qualitatively similar. The nontrivial equilibrium in these regions is stable. In region II, we have a saddle-type equilibrium and there are two main periodic solutions which are created from the Hopf points h_2 and h_4. These periodic solutions undergo sequences of period-doubling bifurcations which are accumulated on the lines PD^1_∞ and PD^2_∞. There are infinitely many periodic solutions produced by the sequences of period-doubling bifurcations. We discuss the dynamics in regions III and IV in the concluding remark.

5.1. Sequence of period-doubling bifurcations

Following the stable periodic solution created at h_2, we find a sequence of period-doubling (PD) and fold (F) bifurcations. Let δ_n be the value where the nth period-doubling bifurcation occurs. For $\beta = -6$, δ_n goes to $2.0511\ldots$, as n goes to infinity. Next we repeat the previously mentioned continuation program for several values of β. In table 1 we have listed the first five values of δ at which the period-doubling occurs for various β and the period T is larger than 45.

Using linear regression, we derive the relation between the above-mentioned accumulation points (δ) with the parameter β, i.e. $\delta = \beta/m_1$ with $m_1 = -2.9252 + \mathcal{O}(10^{-7})$. This is the line labeled as PD^1_∞ in figure 2. Using the same technique, we have constructed the line PD^2_∞ for the sequence of period-doubling bifurcations of the periodic solution created at h_4. The gradient of this line is $-2.5202 + \mathcal{O}(10^{-7})$.

In figure 3 on the left, we have plotted the period of the main periodic solution for fixed $\beta = -6$ against δ. This curve is named $LC1$. We have also plotted a similar curve for the other periodic solution (which is created at the Hopf bifurcation at h_4), namely the curve $LC2$. This situation is in contrast to figure 7 in [23], where the curves $LC1$ and $LC2$ are connected. The curves $LC3$ and $LC5$ are the curves of the period of the periodic solution branching out through period-doubling bifurcations, against δ. The curves are also accumulated into PD^1_∞

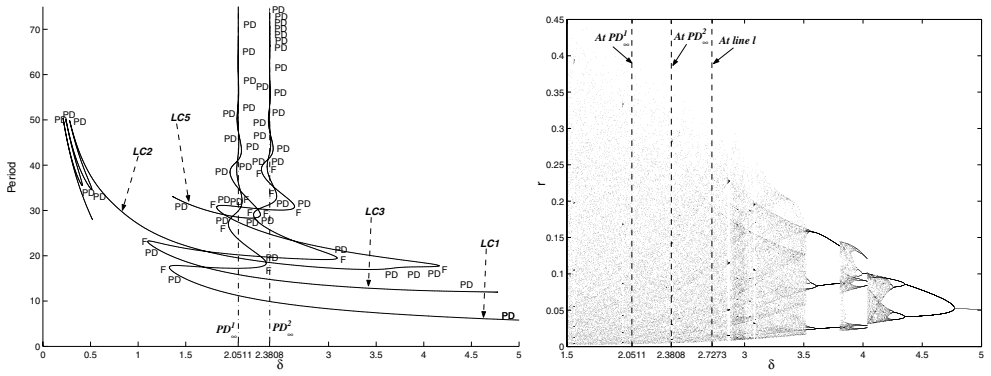

Figure 3. The curves $LC1$ and $LC2$ on the left plot are the periods of the periodic solutions created by Hopf bifurcation at h_2 and h_4 respectively, for $\beta = -6$. The $LC3$ and $LC5$ curves are the periods of the periodic solutions branching out from the first period-doubling bifurcations. On the right is the Poincaré map of the positive attractor projected on the r-axis. On this plot, we have indicated a few locations by dashed lines at which interesting dynamics is expected.

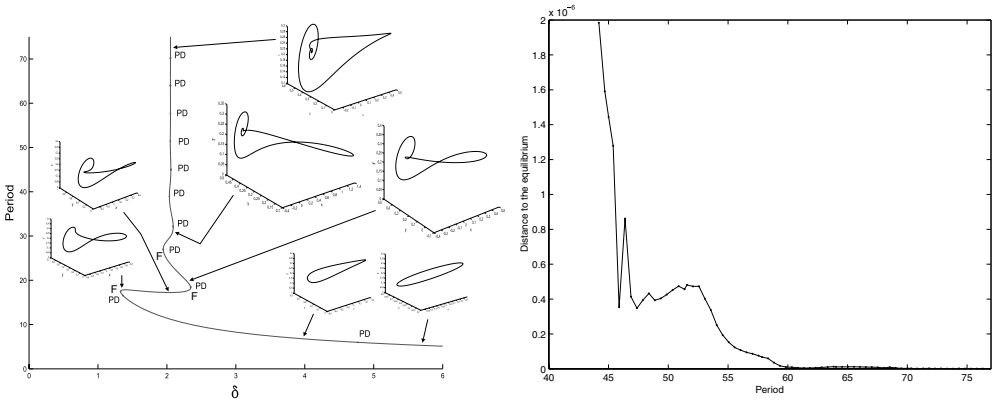

Figure 4. On the left plot we have put together the curve of $LC1$ and some diagrams of periodic solution for different periods. The right plot shows the 'distance' between the periodic solutions to the equilibrium, against the period.

and PD^2_∞. To the right of the previous picture, we have plotted the projection to the r-axis of the positive attractor in the system against the parameter δ.

5.2. The creation of homoclinic orbits

Following the periodic solution on the $LC1$ curve, in figure 4 on the left, we show some diagrams of the periodic solution. From the shape of the periodic solution, there is an indication that a homoclinic orbit is created, as the period goes to infinity. Another evidence is by measuring the distance between the periodic solution to the nontrivial equilibrium. Let φ_T be the T-periodic solution while $\boldsymbol{\xi}_\circ$ is the nontrivial equilibrium. The distance is measured by

$$d(\varphi_T) = \min{}_{0\leqslant t\leqslant T}\{\| \varphi_T(t) - \boldsymbol{\xi}_\circ \|\}.$$

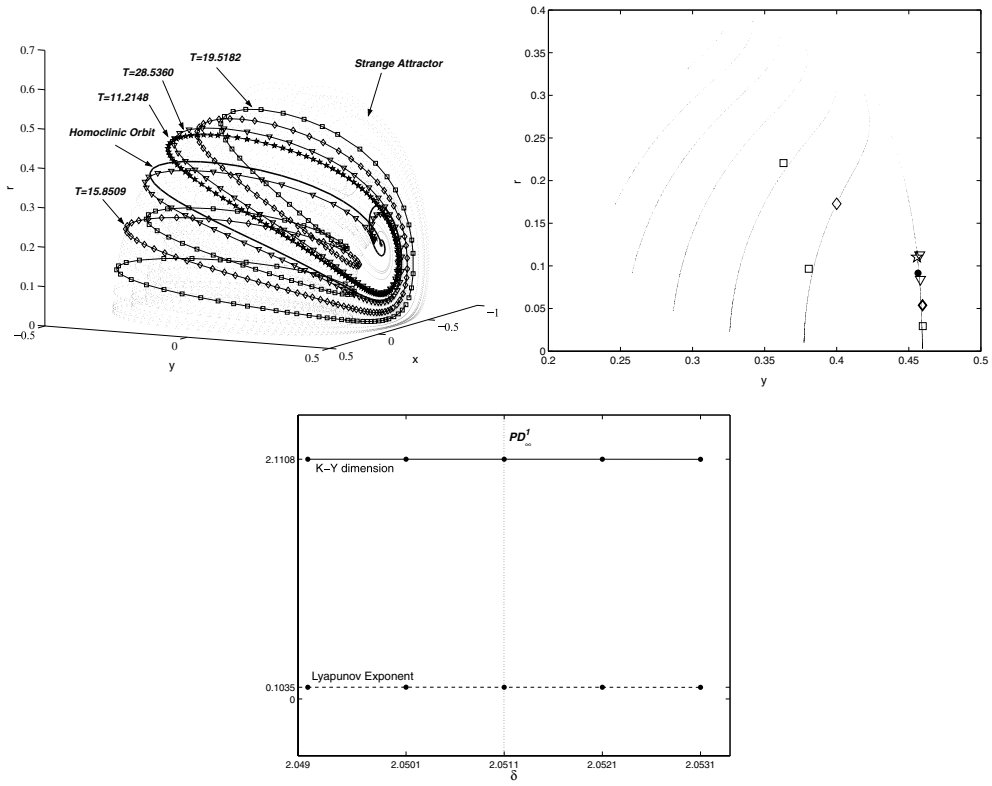

Figure 5. The top left picture is the strange attractors on PD^1_∞ and some periodic solutions which correspond to the curves of periodic solution $LC1$, $LC2$, $LC3$ and $LC5$ in figure 3. The top right picture is the Poincaré section of the strange attractor and the periodic solutions. The bottom picture is the Lyapunov exponent and the Kaplan–Yorke (K–Y) dimension at some point near and at PD^1_∞.

On the right plot in figure 4, we have plotted the function $d(\varphi_T)$ as T goes to infinity. Since the value of $d(\varphi_T)$ goes to zero as T goes to infinity, we conclude that the nontrivial equilibrium collides with the periodic solution. Hence, a homoclinic orbit is created.

5.3. Shil'nikov bifurcation and strange attractor

Following the curve $LC1$, the main periodic solution undergoes infinitely many period-doubling bifurcations. We know that each period-doubling bifurcation creates a new periodic solution with period twice the period of the original one. In general, each of these periodic solutions might undergo a sequence of period-doubling and fold bifurcations. These bifurcations lead to the existence of chaotic dynamics in our system and the creation of a strange attractor.

The strange attractor on the line PD^1_∞ has a positive Lyapunov exponent $0.103\,55\ldots$ and a Kaplan–Yorke (K–Y) dimension $2.110\,76\ldots$. We plot this attractor on figure 5. The mechanism that creates this strange attractor is different from that in [24] (which is via destruction of a torus solution). On the same diagram, we have plotted some periodic solutions and indicated their periods (T). These periodic solutions are computed using the following

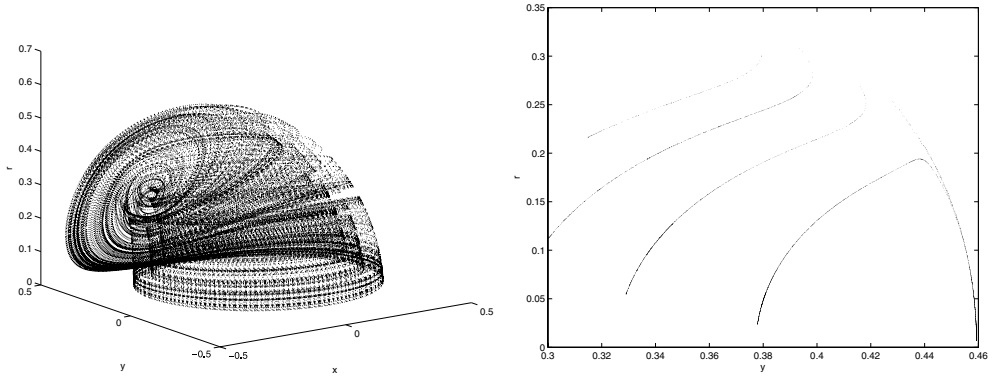

Figure 6. The left picture is the strange attractors on the line l ($\delta = 2.7273\ldots$) for $\beta = -6$. The middle one is the Poincaré section and the right one is the Lyapunov exponent and K–Y dimension.

method. After the nontrivial equilibrium undergoes a Hopf bifurcation, at $\delta = 9.936\,110\ldots$, we follow the periodic solution which is created using the parameter δ. We follow the periodic solution until $\delta = 2.0511\ldots$ is achieved while the period is high enough.

Along the way, the periodic solution undergoes a period-doubling bifurcation. We also follow the new periodic solution using δ until it reaches the same value as previously, and the period is high enough. We repeat this for the two other periodic solutions (which are indicated as $LC3$ and $LC5$ in figure 3).

As is clear from the previous subsection, on the line PD^1_∞ for $\beta = -6$, we have a homoclinic orbit. Moreover the nontrivial equilibrium is a saddle-type equilibrium. The linearized system near this equilibrium has eigenvalues $\Lambda_1 = -1.132$ and $\Lambda_{2,3} = 0.151 \pm 0.499\mathrm{i}$. The above situation satisfies the conditions for Shil'nikov bifurcation. It implies that the system has infinitely many periodic solutions near the value of δ, see [11] for details. Note that the Shil'nikov conditions are also satisfied at PD^2_∞.

The shape of the strange attractor is closely related to the distribution of the periodic solutions. We plot them in figure 5. The stars and the squares form the periodic solutions which have periods 11.2148 and 19.5182. These are the main periodic solutions which lie on the $LC1$. The diamonds and the triangles denote the periodic solutions on the branch $LC3$ and $LC5$ curve in figure 3. Their periods are 15.8509 and 28.5360. We also plot the homoclinic orbit which indicates the Shl'nikov bifurcation in this figure. In figures 6 and 7 we plot two other strange attractors of our system.

The strange attractor which is shown in figure 6 has a Lyapunov exponent $0.107\,097\ldots$ and K–Y dimension $2.14\,146\ldots$. Furthermore, the attractor at $\delta = 2.3808\ldots$ which is shown in figure 7 has a Lyapunov exponent $0.0148\ldots$ with the K–Y dimension $2.019\,87\ldots$. From the Lyapunov exponent and K–Y dimension we see that the strange attractor on the line l is more chaotic than the other two attractors. In figure 7, we see that the attractor has Lyapunov exponent $\mathcal{O}(\varepsilon)$ but the K–Y dimension is ≈ 2. The bifurcation type in this case is not clear at this moment and we leave it for further study.

6. Concluding remarks

An analysis for the dynamics of a singularly perturbed conservative system arising from a system of coupled oscillators at $1 : \varepsilon$ resonance is provided in this paper. As in the previously

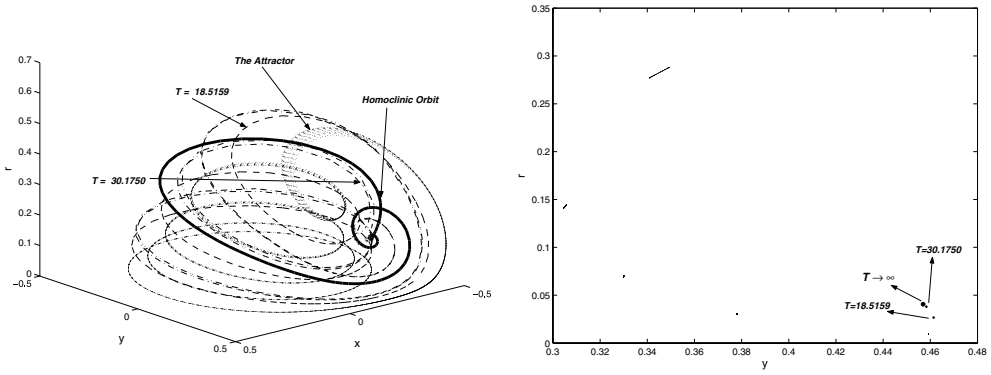

Figure 7. The left picture is the attractor and the homoclinic orbit on the line PD^2_∞ for $\beta = -6$. The middle one is the Poincaré section, and the right one is the Lyapunov exponent and Kaplan–Yorke (K–Y) dimension for some value of δ near $\delta = 2.3808$.

mentioned study, we encounter chaotic dynamics in our system. The mechanism for the creation of chaos in our paper is the sequence of period-doubling bifurcations.

For negative δ, the nontrivial equilibrium is asymptotically stable in region V of figure 2. In other regions, the equilibrium is unstable and most of the solutions are unbounded. Another point to mention is an unstable periodic solution which is created through the Hopf bifurcation on the line h_1. By continuing this periodic solution following the parameter δ, we found a Fold bifurcation at which the periodic solution becomes a saddle type. Using the two-parameter continuation we can compute the fold line, which has a gradient $0.7903 + \mathcal{O}(10^{-10})$ (see figure 2). It is interesting to note that by following this saddle-type periodic solution with δ, the periodic solution becomes large while the period becomes small. Further investigation is necessary to clarify this.

For $\beta = 2\delta$, which is the case of 2:1 resonance which is explained in appendix B, the dynamics of the normal form (B.3) depends only on the ratio of κ_1 and κ_2. For $\beta < 0$ the stability of the equilibrium is shown at $\delta < 0$ in figure 2. To have an asymptotically stable equilibrium, we should choose $\kappa_2/\kappa_1 > 2$. Using our numerical data that we have chosen, the case $\beta = 2\delta$ is located in region III of figure 2. From this result, we conjecture that the exciting dynamics in [23, 24] are there due to the frequencies of the system.

6.1. Application to the atmospheric dynamics

Most of the exciting dynamics observed in [23, 24] are presented here. This suggests that the dynamics which is observed there and also here is a generic phenomenon in our system. A similar dynamics is also observed in the study in [4]. This suggests that our low-dimensional system serves as a good model for the dynamics in [4]. Each oscillator in our system represents a particular dominant flow pattern in atmosphere. These flow patterns are characterized by their frequencies. The parameter in our system namely δ represents the interaction between these flow patterns. The slow–fast dynamics represent the interaction between the flow patterns which have different time scale.

Acknowledgments

The authors wish to thank BPPS-DIKTI for financial support. This research is also supported by ‘Riset ITB 2006 (no. 0004/K01.03.2/PL2.1.5/I/2006)’ and partially by ‘Riset

Internasional ITB 2007 (no. 174/K01.07/PL/2007)'. We wish to thank Ferdinand Verhulst from Universiteit Utrecht for many discussions during this research; also Hendra Gunawan and all members of the Analysis and Geometry Research Group ITB for many comments. F Adi-Kusumo wishes to thank his wife Juwairiah and sons Rizky and Radhya for their special support.

Appendix A. The proof of theorem 3.1

Let us first present two lemmas which will be used for the existence of an equilibrium for system (3.1).

Lemma A.1 [Taylor formula without remainder]**.** *For any C^k-function $f(\boldsymbol{\xi}, \varepsilon)$ there is a C^{k-1}-function $q(\boldsymbol{\xi}, \varepsilon)$, such that $f(\boldsymbol{\xi}, \varepsilon) - f(\boldsymbol{\xi}, 0) = \varepsilon q(\boldsymbol{\xi}, \varepsilon)$ and $q(\boldsymbol{\xi}, 0) = \frac{\partial}{\partial \varepsilon} f(\boldsymbol{\xi}, \varepsilon)$ at $\varepsilon = 0$.*

Proof. Since

$$f(\boldsymbol{\xi}, \varepsilon) - f(\boldsymbol{\xi}, 0) = \int_0^1 \frac{\mathrm{d}}{\mathrm{d}t} \left(f(\boldsymbol{\xi}, t\varepsilon)\right) \mathrm{d}t = \varepsilon \int_0^1 \left.\frac{\partial f(\boldsymbol{\xi}, \eta)}{\partial \eta}\right|_{\eta = t\varepsilon} \mathrm{d}t,$$

we can write $q(\boldsymbol{\xi}, \varepsilon) = \int_0^1 \left.\frac{\partial f(\boldsymbol{\xi}, \eta)}{\partial \eta}\right|_{\eta = t\varepsilon} \mathrm{d}t$. The smoothness of q decreases since the definition involves differentiation. □

Lemma A.2. *Let U be an open subset of $\mathbb{R}^{n+1}$ which consists of points which will be denoted by $(\boldsymbol{\xi}, \varepsilon)$, $(\mathbf{0}, 0) \in U$, $\boldsymbol{f} : U \to \mathbb{R}^n$ is a C^k-mapping. Let*

$$K = \ker(D_{\boldsymbol{\xi}} \boldsymbol{f}(\mathbf{0}, 0)) \quad \text{and} \qquad L = \ker\left(\nabla \left(\frac{\partial}{\partial \varepsilon} f_n(\boldsymbol{\xi}, \varepsilon)\right)\Big|_{(\mathbf{0},0)}\right).$$

We assume that the following holds.

(A_1) $f_n(\boldsymbol{\xi}, 0) = 0$.
(A_2) $\boldsymbol{f}(\mathbf{0}, 0) = \mathbf{0}$.
(A_3) $K \cap L = \{0\}$.

Then we have the following conclusions.

(i) $\dim K = 1, \dim L = n - 1$, *and K and L are complementary linear subspaces of $\mathbb{R}^n$.*
(ii) In a neighborhood of the origin in $\mathbb{R}^n$, the set of $\boldsymbol{\xi}$ such that $\boldsymbol{f}(\boldsymbol{\xi}, 0) = 0$ is a C^k-curve in $\mathbb{R}^n$ through the origin with the tangent space at the origin equal to K.
(iii) There is a C^{k-1}-curve $\gamma : I \to \mathbb{R}^n$, where I is an open interval around 0, and there exists an open neighborhood V of $\mathbf{0}$ in $\mathbb{R}^n$ such that $\gamma(0) = 0$ and, for every nonzero $\varepsilon \in I$, $\gamma(\varepsilon)$ is the unique solution $\xi \in V$ of the equation $\boldsymbol{f}(\boldsymbol{\xi}, \varepsilon) = 0$.

Proof.

(1) From (A_1), we have that $D_{\boldsymbol{\xi}} \boldsymbol{f}(\mathbf{0}, 0)$ has a rank at most $n-1$, which implies that $\dim K \geqslant 1$. Note that

$$\nabla \left(\frac{\partial}{\partial \varepsilon} f_n(\boldsymbol{\xi}, \varepsilon)\right)\Big|_{(\mathbf{0},0)},$$

which is a vector in $\mathbb{R}^n$, can be seen as a linear form. Because L is the kernel of a linear form, $\dim L \geqslant n - 1$. From (A_3) we know that $\dim K + \dim L \leqslant n$. If $\dim K > 1$ then $\dim L < n - 1$, which is a contradiction. Thus $\dim K = 1$ and $\dim L = n - 1$. Furthermore, K and L are complementary linear subspaces of $\mathbb{R}^n$.

(2) Let $\boldsymbol{f}_{n-1}(\boldsymbol{\xi}, \varepsilon)$ denote the first $n-1$ components of $\boldsymbol{f}$. Because of (A_1), the equation $\boldsymbol{f}(\boldsymbol{\xi}, 0) = \mathbf{0}$ is equivalent to $\boldsymbol{f}_{n-1}(\boldsymbol{\xi}, 0) = \mathbf{0}$ (meaning the zero sets of both equations are the same). Moreover,

$$\ker(D_{\boldsymbol{\xi}} \boldsymbol{f}_{n-1}(\mathbf{0}, 0)) = \ker \begin{pmatrix} D_{\boldsymbol{\xi}} \boldsymbol{f}_{n-1}(\mathbf{0}, 0) \\ 0 \ldots 0 \end{pmatrix} = \ker(D_{\boldsymbol{\xi}} \boldsymbol{f}(\mathbf{0}, 0)) = K.$$

From (1) we know that $\dim K = 1$. This means that $D_{\boldsymbol{\xi}} \boldsymbol{f}(\mathbf{0}, 0)$ is surjective. By applying the implicit function theorem we have the result in statement (2).

(3) From the division lemma, there exists a C^{k-1}-function $Q_n(\boldsymbol{\xi}, \varepsilon)$ such that $Q_n(\boldsymbol{\xi}, 0) = \frac{\partial f_n}{\partial \varepsilon}$ at $\varepsilon = 0$ and $f_n(\boldsymbol{\xi}, \varepsilon) = \varepsilon \boldsymbol{Q}_n(\boldsymbol{\xi}, \varepsilon)$. Note that to conclude the latter we have used (A_1), i.e. $f_n(\boldsymbol{\xi}, 0) = 0$. This implies that L is equal to the kernel $D_{\boldsymbol{\xi}} Q_n(0, 0)$. Let us now write

$$\boldsymbol{Q}(\boldsymbol{\xi}, \varepsilon) = \begin{pmatrix} \boldsymbol{f}_{n-1}(\boldsymbol{\xi}, \varepsilon) \\ Q_n(\boldsymbol{\xi}, \varepsilon) \end{pmatrix}.$$

For $\varepsilon \neq 0$ the equation $\boldsymbol{f}(\boldsymbol{\xi}, \varepsilon) = 0$ is equivalent to the equation $\boldsymbol{Q}(\boldsymbol{\xi}, \varepsilon) = 0$. This is clear because, for $Q_n(\boldsymbol{\xi}, \varepsilon) = 0$ is equivalent to $f_n(\boldsymbol{\xi}, \varepsilon) = \varepsilon Q_n(\boldsymbol{\xi}, \varepsilon) = 0$, if $\varepsilon \neq 0$. The kernel of $D_{\boldsymbol{\xi}} \boldsymbol{Q}(\mathbf{0}, 0)$ is equal to the common kernel of $D_{\boldsymbol{\xi}} \boldsymbol{f}_{n-1}(\mathbf{0}, 0)$ and $D_{\boldsymbol{\xi}} Q_n(\mathbf{0}, 0)$, i.e. $K \cap L = \{0\}$. Thus $D_{\boldsymbol{\xi}} \boldsymbol{Q}(\mathbf{0}, 0)$ is invertible and the result in statement (3) follows from the implicit function theorem. □

Proof of the theorem:

Proof. The proof of this theorem follows from lemma A.2, by considering a coordinate transformation

$$\begin{array}{rccl} T: & \xi_j & \mapsto & \zeta_j = \xi_j + \xi_{\circ j} \\ & \xi_n & \mapsto & \zeta_n = H(\xi) - H(\boldsymbol{\xi}_\circ). \end{array}$$

The origin of the new coordinate system corresponds to $\boldsymbol{\xi}_\circ$. In this new coordinate we have a system of ordinary differential equations $\dot{\boldsymbol{\zeta}} = \tilde{\boldsymbol{F}}(\boldsymbol{\zeta}, \varepsilon)$ where $\tilde{F}_n(\zeta, \varepsilon) = (\nabla H(\boldsymbol{\xi}(\boldsymbol{\zeta})))^T \boldsymbol{F}(\boldsymbol{\xi}(\boldsymbol{\zeta}), \varepsilon)$. Clearly $\tilde{F}_n(\zeta, 0) = 0$, for all $\boldsymbol{\zeta}$ since H is an integral of $\boldsymbol{F}^\circ(\xi) = \boldsymbol{F}(\boldsymbol{\xi}, 0)$. The theorem then follows from (A.2). □

Appendix B. The 2:1 resonance case of the system in [23]

In this section, we will show that the normal form of the system in [23] at 2:1 resonance is contained in the system (2.1).

Recall the system in [23]:

$$\dot{\boldsymbol{\xi}} = \begin{pmatrix} D_1 & 0 \\ 0 & D_2 \end{pmatrix} \boldsymbol{\xi} + \tilde{\varepsilon} \boldsymbol{F}(\boldsymbol{\xi}), \qquad 0 < \tilde{\varepsilon} \ll 1, \tag{B.1}$$

with $\boldsymbol{\xi} \in \mathbb{R}^4$ and $\boldsymbol{F} : \mathbb{R}^4 \to \mathbb{R}^4$. The function $\boldsymbol{F}$ is assumed to be a quadratic, homogeneous polynomial in $\boldsymbol{\xi}$ satisfying $\boldsymbol{\xi} \cdot \boldsymbol{F}(\boldsymbol{\xi}) = 0$. We assume that D_j, $j = 1, 2$, are 2×2 matrices with eigenvalues $\tilde{\varepsilon}\mu_1 \pm \mathrm{i}$ and $\tilde{\varepsilon}\mu_2 \pm \mathrm{i}(2 + \omega)$, respectively. Here μ_1 and μ_2 are $O(1)$ while ω is $\mathcal{O}(\tilde{\varepsilon})$, known as the detuning parameter. The system (B.1) can then be viewed as a system of coupled oscillators near $2:1$ resonance, with dissipation. To apply the averaging method, we transform

$$\begin{aligned} &\xi_1 \mapsto r_1 \cos(t + \varphi_1), \qquad && \xi_2 \mapsto -r_1 \sin(t + \varphi_1), \\ &\xi_3 \mapsto r_2 \cos(2t + \varphi_2), \qquad && \xi_4 \mapsto -r_2 \sin(2t + \varphi_2) \end{aligned}$$

and then average the resulting equations of motion with respect to t over 2π. According to the averaging theorem (see Sanders and Verhulst [17]), the solution of the averaged equations and the original equations for the same initial condition stay in the $\mathcal{O}(\varepsilon)$-neighborhood of each other for $\mathcal{O}(1/\varepsilon)$ time scale. One should of course carefully check the boundedness condition in the theorem. In our case they are satisfied.

Thus, the averaged system:

$$\begin{aligned}
\dot{r}_1 &= \tilde{\varepsilon}\,(\mu_1 r_1 + r_1 r_2(\delta_1 \sin(2\varphi_1 - \varphi_2) + \delta_2 \cos(2\varphi_1 - \varphi_2)))\\
\dot{r}_2 &= \tilde{\varepsilon}\,\left(\mu_2 r_2 + r_1^2(-\delta_1 \sin(2\varphi_1 - \varphi_2) - \delta_2 \cos(2\varphi_1 - \varphi_2))\right)\\
\dot{\varphi}_1 &= \tilde{\varepsilon} r_2\,(-\delta_2 \sin(2\varphi_1 - \varphi_2) + \delta_1 \cos(2\varphi_1 - \varphi_2))\\
\dot{\varphi}_2 &= \tilde{\varepsilon}\left(\omega + \frac{-\delta_2 r_1^2 \sin(2\varphi_1 - \varphi_2) + \delta_1 r_1^2 \cos(2\varphi_1 - \varphi_2)}{r_2}\right)
\end{aligned} \tag{B.2}$$

serves as an $\mathcal{O}(\varepsilon)$ approximation for the original system on a time scale of $1/\varepsilon$. The parameters δ_1 and δ_2 are dependent on the coefficients of $\boldsymbol{F}$.

Further simplification of (B.2) can be done by defining $\varphi = 2\varphi_1 - \varphi_2$ which reduces the dimension by 1. This is typical for autonomous system after averaging. The reduced averaged equations are

$$\begin{aligned}
\dot{r}_1 &= \varepsilon\,(\mu_1 r_1 + r_1 r_2(\delta_1 \sin(\varphi) + \delta_2 \cos(\varphi)))\\
\dot{r}_2 &= \varepsilon\,\left(\mu_2 r_2 + r_1^2(-\delta_1 \sin(\varphi) - \delta_2 \cos(\varphi))\right)\\
\dot{\varphi} &= \varepsilon\left(\left(-2\delta_2 r_2 + \frac{\delta_2 r_1^2}{r_2}\right)\sin(\varphi) + \left(2\delta_1 r_2 - \frac{\delta_1 r_1^2}{r_2}\right)\cos(\varphi) - \omega\right).
\end{aligned}$$

Let us transform the system into Cartesian coordinate by defining $r = r_1$, $u = r_2 \cos\varphi$ and $v = r_2 \sin\varphi$. The transformed system is

$$\begin{aligned}
\dot{r} &= \varepsilon(\mu_1 r + (\delta_1 v + \delta_2 u)r)\\
\dot{u} &= \varepsilon(\mu_2 u + 2(\delta_2 v - \delta_1 u)v - \delta_2 r^2 + \omega v)\\
\dot{v} &= \varepsilon(\mu_2 v - 2(\delta_2 v - \delta_1 u)u - \delta_1 r^2 - \omega u).
\end{aligned}$$

Lastly, we define a transformation: $(r, u, v) \longmapsto (r, x, y)$ with $x = (\delta_1 v + \delta_2 u)/\delta$, $y = (\delta_2 v - \delta_1 u)/\delta$, which is a rotation with respect to the r-axis. By doing this, the normal form can be written as (after re-scaling time $t \mapsto \varepsilon t$)

$$\begin{pmatrix}\dot{r}\\ \dot{x}\\ \dot{y}\end{pmatrix} = \begin{pmatrix}\mu_1 & 0 & 0\\ 0 & \mu_2 & 0\\ 0 & 0 & \mu_2\end{pmatrix}\begin{pmatrix}r\\ x\\ y\end{pmatrix} + \begin{pmatrix}\delta x r\\ \Omega y - \delta r^2\\ -\Omega x\end{pmatrix}. \tag{B.3}$$

with $\Omega = 2\delta y + \omega$. One can see that by setting $\mu_1 = \varepsilon\kappa_1$ and $\mu_2 = -\varepsilon\kappa_2$ for $\kappa_1, \kappa_2 > 0$, we arrive at the system (2.1) for $\beta = 2\delta$.

References

[1] Arnol'd V I 1978 *Mathematical Methods of Classical Mechanics* (New York: Springer)

[2] Broer H W, Chow S N, Kim Y and Vegter G 1993 A normally elliptic Hamiltonian bifurcation *Z. Angew. Math. Phys.* **44** 389–432

[3] Broer H W, Chow S N, Kim Y and Vegter G 1995 The Hamiltonian double-zero eigenvalue *Field Inst. Commun.* **4** 1–19

[4] Crommelin D T 2002 Homoclinic dynamics: a scenario for atmospheric ultralow-frequency variability *J. Atmos. Sci.* **59** 1533–49

[5] Dhooge A, Govaerts W and Kuznetsov Y A 2003 MATCONT: a MATLAB package for numerical bifurcation analysis of ODEs *ACM Trans. Math. Softw.* **29** 141–64

[6] Fatimah S and Ruijgrok M 2002 Bifurcation in autoparametric system in 1:1 internal resonance with parametric excitation *Int. J. Non-Linear Mech.* **37** 297–308
[7] Fenichel N 1979 Geometric singular perturbation theory for ordinary differential equations *J. Differ. Equ.* **31** 53–98
[8] Guillemin V and Pollack A 1974 *Differential Topology* (Englewood Cliffs, NJ: Prentice-Hall)
[9] Haller G 1999 *Chaos Near Resonance (Applied Mathematical Sciences vol 138)* (New York: Springer)
[10] Hirsch M W 1994 *Differential Topology (Graduate Texts in Mathematics vol 33)* (New York: Springer) (Corrected reprint of the 1976 original)
[11] Kuznetsov Y A 1998 *Elements of Applied Bifurcation Theory (Applied Mathematical Sciences vol 112) 2nd edn* (New York: Springer)
[12] Langford W F and Zhan K 1999 Interaction of Andronov-Hopf and Bogdanov-Tekens Bifurcation *Field Inst. Commun.* **24** 365–83
[13] Langford W F and Zhan K 1999 *Hopf Bifurcation Near 0:1 Resonance Proc. BTNA'98* eds Chen, Chow and Li (New York: Springer) pp 1–18
[14] Nayfeh S A and Nayfeh A H 1993 Nonlinear interaction between two widely spaced modes-external excitation *Int. J. Bifurcat. Chaos* **3** 417–27
[15] Nayfeh A H and Malatkar P 2003 On the transfer of energy between widely spaced modes in structures *Nonlinear Dyn.* **31** 225–42
[16] Sanders J A 1978 Are higher order resonances really interesting? *Celestial Mech.* **16** 421–40
[17] Sanders J A and Verhulst F 1985 *Averaging Methods in Nonlinear Dynamical System (Appl. Math. Sciences vol 59)* (New York: Springer)
[18] Stiefenhofer M 1998 Singular perturbation with limit points in the fast dynamics *Z. Angew. Math. Phys.* **49** 730–58
[19] Tondl A, Ruijgrok M, Verhulst F and Nabergoj R 2000 *Autoparametric Resonance in Mechanical Systems* (New York: Cambridge University Press)
[20] Tuwankotta J M and Verhulst F 2000 Symmetry and resonance in Hamiltonian systems *SIAM J. Appl. Math.* **61** 1369–85
[21] Tuwankotta J M 2002 Heteroclinic behaviour in a singularly perturbed conservative system *Higher-Order Resonances in Dynamical Systems PhD Thesesat* Utrecht University, http://www.library.uu.nl/digiarchief/dip/diss/2003-0114-104617/inhoud.htm
[22] Tuwankotta J M and Verhulst F 2003 Hamiltonian system with widely separated frequencies *Nonlinearity* **16** 689–706
[23] Tuwankotta J M 2003 Widely separated frequencies in coupled oscillators with energy-preserving quadratic nonlinearity *Physica* D **182** 125–49
[24] Tuwankotta J M 2006 Chaos in coupled ocsillators with widely separated frequencies and energy-preserving nonlinearity *Int. J. Nonlinear Mech.* **41** 180–91